Journal of Mining Science, Vol. 44, No. 3, 2008

GEOMECHANICS

EFFECT OF VISCOSITY OF PARTINGS IN BLOCK-HIERARCHICAL MEDIA ON PROPAGATION OF LOW-FREQUENCY PENDULUM WAVES

N. I. Aleksandrova, E. N. Sher, and A. G. Chernikov UDC 539.375

The study focuses on the pendulum-type wave propagation in an assembly of steel rods parted alternatively by rubber and foam plastic and exposed to impulse loading. The proposed numerical model describes this system as a chain of masses linked by elastic springs and viscous damping elements. At large times from the loading onset, the asymptotical estimates of velocities and accelerations of the masses are obtained. The numerical calculations, analytical solutions and experimental data are compared, and the domain of applicability of the analytical evaluations is delimited. The authors show that this model adequately describes perturbations in the system of rods with alternating visco-elastic partings.

Impact, block hierarchical medium, seismic waves, pendulum-type waves, partings, elasticity, viscosity

The contemporary geomechanical and geophysical sciences describe deformation of a rock mass as of a complex hierarchy of block structures. As per this concept, a rock mass is a system of various scale blocks embodied into one another [1, 2]. Inter-block layers are usually composed of weaker and fissured rocks, and, based on that, deformation of a block rock mass, both statically and dynamically, occurs due to deformation of these partings.

The theoretical and experimental studies into the waveguide properties of one-dimensional block models in the form of chains of elastic blocks with friable layers in between them showed that wave propagation in such media is sufficiently described by an approximation that the blocks are non-deformable bodies. And the low-frequency pendulum-type waves that arise under an impact action are cleanly enough represented in this case [3 – 7]. We know from experiments that high-frequency waves peculiar for natural oscillations of blocks attenuate rather quickly. A good compliance of the theory and experiment is reached in a visco-elastic model of the partings [8, 9].

This article is a study into the damping effect of the partings of blocks on the propagation of non-stationary waves in periodical block hierarchies.

EXPERIMENTAL STUDY OF WAVE PROPAGATION IN ONE-DIMENSIONAL BLOCK MODEL

An assembly of steel rods with a length $l = 0.1$ m and weight $m = 0.3822$ kg, parted with different materials was tested. The rods were installed into a vertical tube with lengthwise cuts for cables of accelerometers KD-91 built lengthwise in the 3rd, 4th, 5th, 12th and 13th rod, in the upper part. The free upper-rod face was impacted with a force read by an accelerometer attached to the hammer head. Due to the 2 m length of the assembly, it was possible to register oscillations of the rods prior to the arrival of reflected waves from the lower face of the assembly by analog-to-digital converter E-440 for simplifying the data processing and, in particular, FFT.

Institute of Mining, Siberian Branch, Russian Academy of Sciences, E-mail: vzryvlab@misd.nsc.ru, Novosibirsk, Russia. Translated from Fiziko-Tekhnicheskie Problemy Razrabotki Poleznykh Iskopaemykh, No. 3, pp. 3-13, May-June, 2008. Original article submitted March 20, 2008.

1062-7391/08/4403-0225

Characteristic experimental oscillograms of rock accelerations $\ddot{u}_j(t)$ (j is a number of a mass) and their spectral densities $G_j(\omega) = \left| \int_0^T \ddot{u}_j(t)\, e^{-i\omega t} dt \right|$ plotted for systems with different partings are shown as solid lines in Figs. 1 – 3, where dashes and thin solid lines depict the theoretical calculations described below. Figures 1 and 2 illustrate the data obtained in the 4th and 12th rods parted by foam plastic and porous rubber, respectively; and acceleration oscillograms and spectral densities plotted for the 3rd and 13th rods parted alternatively by foam plastic and porous rubber are in Fig. 3. This experiment agrees with modeling wave propagation in a second-order hierarchical medium [10], where blocks contain sub-blocks as in Born's chain.

Figures 1 and 2 show the propagation of an impact-excited low-frequency pendulum-type wave in the first-order rod system (no sub-blocks). The properties of partings govern the pendulum wave speed, spectral composition and attenuation coefficient. The rod system with foam plastic partings has the maximum propagation speed (114 m/s), wide frequency band (to 300 Hz) and weak attenuation as compared with the rods parted by porous rubber, where the wave propagation speed is 77 m/s, frequency band is up to 230 Hz. The rods parted alternatively by foam plastic and porous rubber, as a prototype of Born's chain, are characterized by the more complex wave behavior (Fig. 3). Two waves, low-frequency pendulum wave followed by high-frequency pendulum wave, are observed in the first rods. While propagating, the high-frequency wave attenuates quickly, unlike in a system of elastic springs [10], and is absent on the 13th rod already; only the low-frequency pendulum wave is recorded with its propagation speed of 65 m/s, which is less than in the porous rubber parted rod system. Accordingly, the wave pattern in the first rods has two maximums for two waves. It is seen that in the propagating high-frequency wave, the amplitude weakens quicker than the amplitude in the low-frequency wave, and there is no second maximum in the 13th rod.

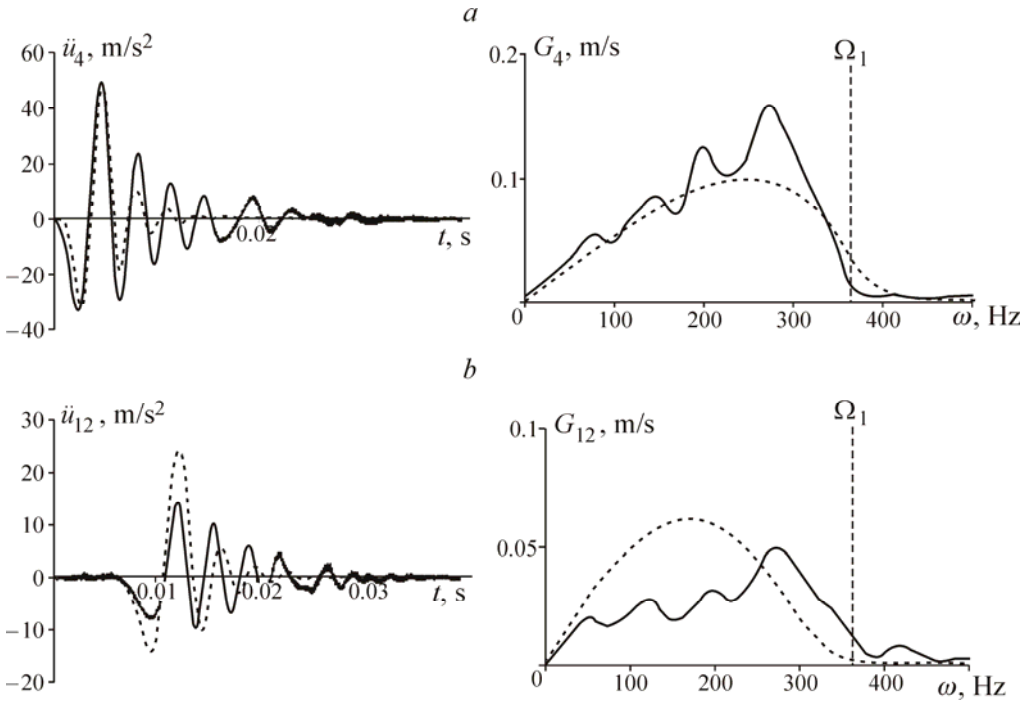

Fig. 1. Acceleration oscillograms for (*a*) 4th and (*b*) 12th rod and their spectral densities in a system of rods with foam plastic partings exposed to impact loading

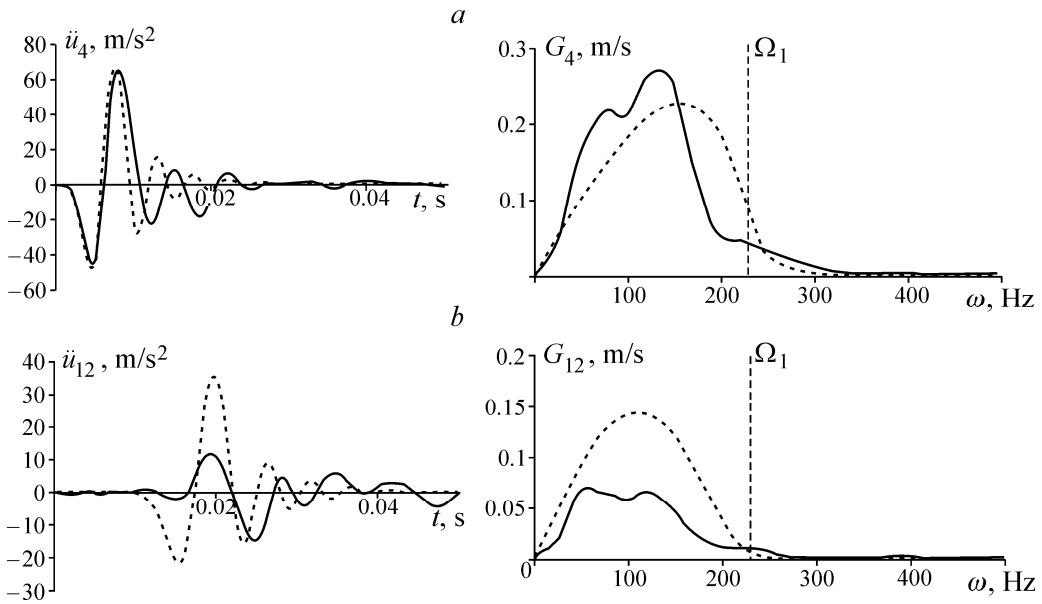

Fig. 2. Acceleration oscillograms of (*a*) 4th and (*b*) 12th rods and their spectral densities under blowing a system of rods with porous rubber partings

We have experimentally obtained that energy dissipation in the partings influences largely the wave propagation in a block system, which calls for theoretical modeling of this process. Visco-elastic behavior of partings is one of the causes of energy dissipation, which has successfully been taken into account in modeling wave propagation in one-dimensional chain of masses with two couples of elastic and damping elements inserted in line or in parallel [8, 9]. We analyzed theoretically a model with partings and parallel arranged elastic and damping elements.

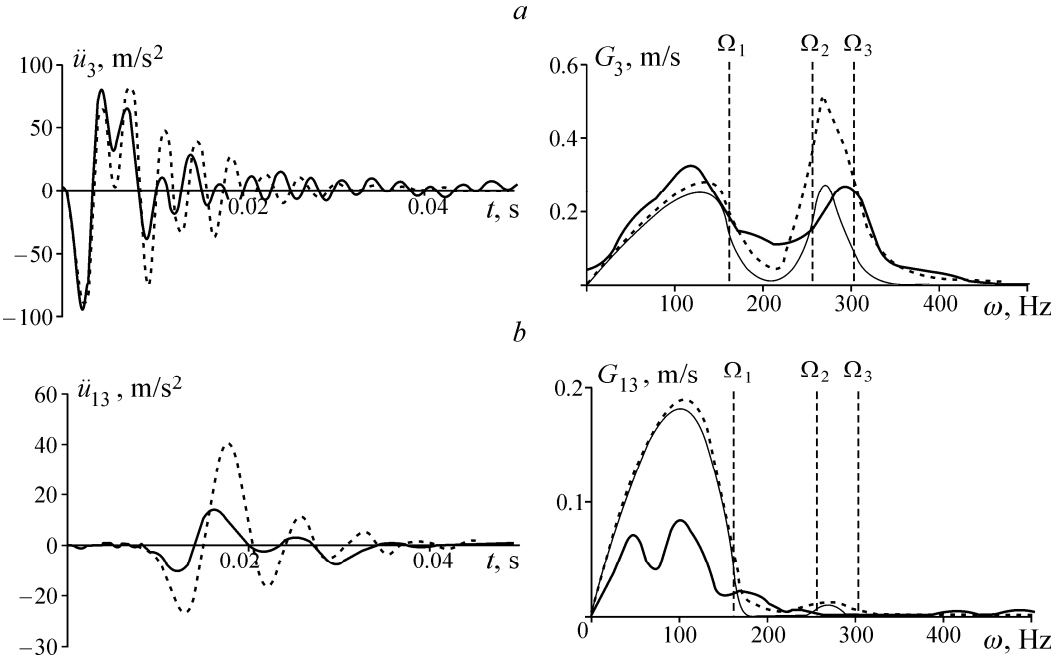

Fig. 3. Acceleration oscillograms of (*a*) 3rd and (*b*) 13th rod and their spectral density for the case when an impact is performed on a chain of rods parted in turn by foam plastic and porous rubber

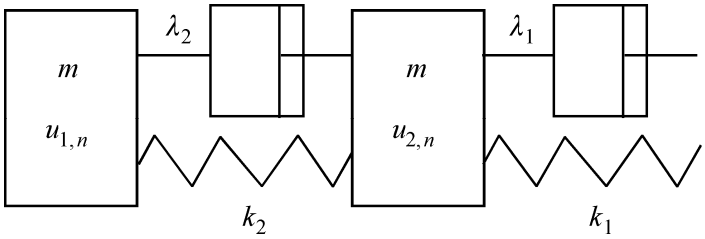

Fig. 4. Scheme of a model of the second order hierarchic system of visco-elastically linked masses, 2*l* in length

Problem Statement. The problem covers a chain of masses interlinked by visco-elastic layers as in Fig. 4. A system of masses with two types of partings arranged in turn is described by motion equations as below:

$$m\ddot{u}_{1,n} = k_2(u_{2,n} - u_{1,n}) - k_1(u_{1,n} - u_{2,n-1}) + \lambda_2(\dot{u}_{2,n} - \dot{u}_{1,n}) - \lambda_1(u_{1,n} - \dot{u}_{2,n-1}),\ n = 2, ..., N,$$

$$m\ddot{u}_{2,n} = -k_2(u_{2,n} - u_{1,n}) + k_1(u_{1,n+1} - u_{2,n}) - \lambda_2(\dot{u}_{2,n} - \dot{u}_{1,n}) + \lambda_1(u_{1,n+1} - \dot{u}_{2,n}),\ n = 1, ..., N-1, \qquad (1)$$

$$m\ddot{u}_{1,1} = k_2(u_{2,1} - u_{1,1}) + \lambda_2(\dot{u}_{2,1} - \dot{u}_{1,1}) + Q(t),\quad u_{2,N} = 0.$$

Here, $u_{1,n}$ and $u_{2,n}$ are displacements of the first and second masses, respectively, in an n-th block; k_1 and k_2 are spring stiffnesses; λ_1 and λ_2 are viscosities of damping elements; m is a mass; l is a distance between masses. Initial conditions are zero. The chain end mass is rigidly fixed. At $t = 0$ the first mass is affected with a half-sine force with an amplitude P_0:

$$Q(t) = P_0 \sin(\omega_* t) H_0(\pi - \omega_* t) H(t), \qquad (2)$$

where ω_* is an impact frequency; H is Heaviside's function. The difference between this system and Born's chain from [10] is the damping elements.

Dashed curves in Figs. 1 – 3 are for the finite-difference method solution of (1), (2) by an explicit scheme. Connection between the numbers of masses, *j*, in the chain, of block *n* and of mass *k* in the blocks is by the formula: $j = 2n - 2 + k$. Viscosity and stiffness parameters of different partings for numerical modeling were chosen on the basis that a pendulum wave propagation speed and its period velocity coincide in the vicinity of the wave front, as per the experiments on homogenous systems (Figs. 1 and 2). The value of ω_* was also experimentally obtained. Thus, for porous rubber partings: $\lambda_1 = \lambda_2 = 20$ kg/s, $k_1 = k_2 = 0.2 \cdot 10^6$ kg/s^2, $\omega_* = 3.14$ Hz; for foam plastic partings: $\lambda_1 = \lambda_2 = 35$ kg/s, $k_1 = k_2 = 0.5 \cdot 10^6$ kg/s^2, $\omega_* = 13.66$ Hz. Numerical calculations for an assembly interlaid with foam plastic and porous rubber partings were performed with the same viscous and stiff parameters as of homogenous systems: $\lambda_1 = 20$ kg/s, $\lambda_2 = 35$ kg/s $k_1 = 0.2 \cdot 10^6$ kg/s^2, $k_2 = 0.5 \cdot 10^6$ kg/s^2, the only difference was $\omega_* = 15.71$ Hz. The other calculation parameters were the same as per the experiment: $l = 0.1$ m, $m = 0.3822$ kg, $\tau = 0.001$ ms (τ is a time step of the difference scheme). Comparison of the numerical and experimental curves shows that the chain model of the visco-elastically linked masses gives a good description of the experimental oscillograms and spectra at

short distances from the point of attack (3rd – 5th rods). At long distances the experimental pendulum wave amplitude decays markedly stronger that the calculated one, though there is no mismatch in the wave propagation speed and the signal shape. This circumstance means that the question of energy dissipation during wave propagation in a block-structured medium needs a more profound research, and the theoretical model should be improved.

Asymptotic Estimates. The analytical solution to be obtained, let the chain of masses be infinite. Applying the Laplace transform in time and the Fourier transform in longitudinal coordinate n (ρ and q are the corresponding parameters) to a system of equations (1) with force (2) yields the solution in as the Laplace – Fourier representation:

$$u_1^{LF_d} = \frac{Q^L[p^2 + p(\lambda_1 + \lambda_2)/m + (k_1 + k_2)/m]}{mD(p,q)}, \quad u_2^{LF_d} = \frac{Q^L[(\lambda_1 p + k_1)e^{-2iql} + (\lambda_2 p + k_2)]}{mD(p,q)},$$

$$D(p,q) = p^4 + \frac{2}{m}p^2(\lambda_1 p + k_1 + \lambda_2 p + k_2) + \frac{4}{m^2}(\lambda_1 p + k_1)(\lambda_2 p + k_2)\sin^2(ql).$$

Here, $D(p,q)$ is a dispersion operator of the system.

Analyzing equation $D(iqc,q) = 0$, we study the first two modes of the dispersion curves. Figure 5 shows the relationships of modes I and II of the frequency $\omega = qc$, phase and group velocities and the wave number q, calculated with the same parameters as in Fig. 3. Similarly to the case of no viscosity ($\lambda_1 = \lambda_2 = 0$) [10], there are two frequency cut-off zones (propagation of harmonic waves with such frequencies is impossible): $\Omega_1 \le \omega \le \Omega_2$ and $\omega \ge \Omega_3$, where Ω_1, Ω_2 at low viscous parameters coincide with high accuracy with the analogous values for Born's chain without damping elements [10]:

$$\Omega_{1,2} \approx \Omega_0\sqrt{1 \pm \sqrt{1-\beta}}, \quad \Omega_0 = \sqrt{\frac{k_1+k_2}{m}}, \quad \Omega_3 = \sqrt{\frac{2(k_1+k_2)}{m} - \frac{(\lambda_1+\lambda_2)^2}{m^2}}, \quad \beta = \frac{4k_1k_2}{(k_1+k_2)^2}. \qquad (3)$$

The vertical dashed lines in the spectral density graphs in Fig. 3 and horizontal dashed line in Fig. 5 correspond to Ω_1, Ω_2, Ω_3 calculated from (3). Analysis of the graphs shows a concordance of estimates (3) and both the experimental and theoretical spectra obtained with the finite-difference method.

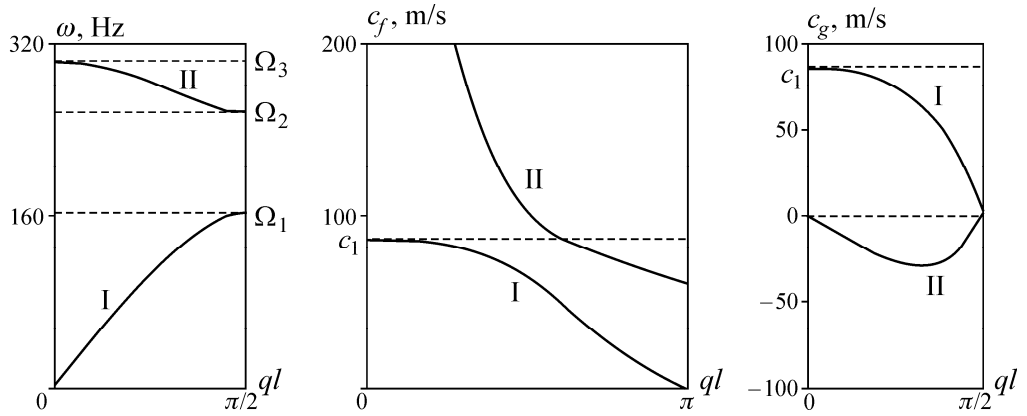

Fig. 5. Dispersion curves

Analysis of $c(q)$ produced the formulas below to find asymptotics of the infinite-long waves $(q \to 0)$:

$$c = c_1(1-\alpha q^2), \quad c_1 = l\sqrt{\frac{2k_1k_2}{(k_1+k_2)m}}, \quad \alpha = \frac{l^2}{6}(1-3\delta), \tag{4}$$

$$\delta = -\frac{(k_1+k_2)m}{k_1k_2}\left\{\alpha_1{}^2\left(10+\frac{4(k_1+k_2)m}{(\lambda_1+\lambda_2)^2}\right)-\frac{8\alpha_1}{m}\left(\frac{\lambda_1\lambda_2}{\lambda_1+\lambda_2}+\frac{\lambda_1k_2+\lambda_2k_1}{k_1+k_2}-\frac{k_1k_2m}{(k_1+k_2)(\lambda_1+\lambda_2)}\right)-\right.$$
$$\left.-\frac{4(\lambda_1k_2+\lambda_2k_1)}{m^2(k_1+k_2)}\left(\frac{2\lambda_1\lambda_2}{\lambda_1+\lambda_2}-\frac{(\lambda_1k_2+\lambda_2k_1)m}{(\lambda_1+\lambda_2)^2}\right)\right\}, \quad \alpha_1 = \frac{(\lambda_1k_2^2+\lambda_2k_1^2)}{m(k_1+k_2)^2}.$$

Evident is the independence of velocity c_1 of long-wave excitations forming a quasi-front from the viscosity of damping elements.

Using Slepyan's method of inverse of two-to-one integral transforms in the vicinity of the ray $x = c_1t$ [11], we have obtained the asymptotics of low-frequency excitations near the quasi-front $x = c_1t$ at infinitely large time from the process onset:

$$\ddot{u}_{k,n} = \frac{2P_0c_1l}{m\omega_*(\gamma t)^{2/3}}\frac{1}{\pi}\int_0^\infty \sin(æ_k z + z^3/3)e^{-\mu z^2}z\,dz,$$
$$\dot{u}_{k,n} = \frac{2P_0l}{m\omega_*(\gamma t)^{1/3}}\frac{1}{\pi}\int_0^\infty \cos(æ_k z + z^3/3)e^{-\mu z^2}\,dz, \quad k = 1, 2; \tag{5}$$
$$æ_1 = \frac{(2n-2)-c_1t}{(\gamma t)^{1/3}}, \quad æ_2 = \frac{(2n-1)-c_1t}{(\gamma t)^{1/3}}, \quad \gamma = 3c_1\alpha, \quad \mu = \frac{\alpha_1l^2t}{(\gamma t)^{2/3}}.$$

When $\lambda_1 = \lambda_2 = 0$, there is no an exponential factor under integrals $(\mu = 0)$ and formulas (5) take on the form of:

$$\ddot{u}_{k,n} = \frac{2P_0c_1l}{m\omega_*(\gamma t)^{2/3}}\frac{d\mathrm{Ai}(æ_k)}{dæ_k}, \quad \dot{u}_{k,n} = \frac{2P_0l}{m\omega_*(\gamma t)^{1/3}}\mathrm{Ai}(æ_k), \quad k = 1,2; \tag{6}$$
$$\gamma = \frac{c_1l^2}{2}\left(1-\frac{3}{4}\beta\right), \quad \mathrm{Ai}(æ) = \frac{1}{\pi}\int_0^\infty \cos(æz + z^3/3)dz.$$

Here, Ai is Airy's function [2]. When the viscosity is zero, lowering of the maximal acceleration amplitude near the quasi-front as the number of a block grows is proportional to $n^{-2/3}$, the same decrease for the velocities is proportional to $n^{-1/3}$:

$$\max_t \ddot{u}_{1,n} = \frac{0.52\,P_0c_1}{m\omega_*l}(2n-2)^{-2/3}, \quad \max_t \dot{u}_{1,n} = \frac{1.07\,P_0}{m\omega_*}(2n-2)^{-1/3}, \quad n \to \infty.$$

The viscosity present causes higher damping. When $\lambda_1, \lambda_2 \neq 0$ and $n \to \infty$ at the same time, formulas (5) get simpler:

$$\dot{u}_{k,n} = \frac{P_0}{m\omega_*\sqrt{\pi\alpha_1 t}}\exp\left(-\frac{\tilde{æ}_k^2}{4}\right), \quad \ddot{u}_{k,n} = \frac{P_0c_1}{m\omega_*\alpha_1l\sqrt{\pi}}\frac{\tilde{æ}_k}{t}\exp\left(-\frac{\tilde{æ}_k^2}{4}\right), \quad k = 1, 2; \tag{7}$$
$$\tilde{æ}_1 = \frac{(2n-2)l-c_1t}{l\sqrt{\alpha_1 t}}, \quad \tilde{æ}_2 = \frac{(2n-1)l-c_1t}{l\sqrt{\alpha_1 t}}.$$

The decrease of the maximal amplitudes of the velocities of masses is proportional to $t^{-1/2}$, the same decrease for the accelerations is proportional to t^{-1}:

$$\max_t \dot{u}_n = \frac{P_0}{m\omega_*\sqrt{\pi\alpha_1 t}}, \quad \max_t \ddot{u}_n = \frac{P_0 c_1}{\omega_* m l \alpha_1 t\sqrt{2\pi\,\mathrm{e}}}, \quad n \to \infty .$$

It follows from a comparison with an analytical solutions obtained for homogenous assembly [8] that with high viscosity parameters $\lambda_1, \lambda_2 \neq 0$ and when $n \to \infty$ the long-wave excitations behave in the same way as in the equivalent homogenous assembly with the reduced stiffness k and viscosity λ:

$$k = \frac{2k_1k_2}{k_1 + k_2}, \quad \lambda = 2m\alpha_1 = \frac{2(\lambda_1 k_2^2 + \lambda_2 k_1^2)}{(k_1 + k_2)^2}.$$

If partings have low or no viscosity, the equivalent homogenous assembly parameters are found based on the condition of equality of long wave velocities and coefficient α in formulae (4):

$$k = \frac{k_1k_2}{4\sqrt{k_1^2 - k_1k_2 + k_2^2}}, \quad l = 2l\sqrt{1 - \frac{4k_1k_2}{3(k_1 + k_2)^2}}.$$

With the purpose of deriving the analytical expression for the spectral density, we apply the transform $f^{\tilde{L}} = \int_0^\infty f(t)e^{-i\omega t}dt$ to (1) and (2). The linear system of equations yields expressions for representation of the displacements:

$$\ddot{u}_{k,n}^{\tilde{L}} = \frac{Q^{\tilde{L}} R_k \omega^2 e^{-2i\gamma n}}{(k_1 + i\omega\lambda_1)F}, \quad k = 1, 2; \tag{8}$$

$$R_1 = (k_1 + i\omega\lambda_1)e^{2i\gamma} + k_2 + i\omega\lambda_2, \quad R_2 = -m\omega^2 + k_1 + i\omega\lambda_1 + k_2 + i\omega\lambda_2,$$

$$F = -m\omega^2 e^{2i\gamma} + (k_1 + i\omega\lambda_1)(e^{2i\gamma} - 1),$$

where γ is the solution of the equation below:

$$\cos 2\gamma = 1 - A + iB,$$

$$A = \frac{\omega^2 m[\omega^4 m\lambda_1\lambda_2 + \omega^2\{2(\lambda_1^2k_2 + \lambda_2^2k_1) - mk_1k_2\} + 2(k_1 + k_2)k_1k_2]}{2(k_1^2 + \omega^2\lambda_1^2)(k_2^2 + \omega^2\lambda_2^2)},$$

$$B = \frac{\omega^3 m[\omega^2\{2\lambda_1\lambda_2(\lambda_1 + \lambda_2) - m(\lambda_1k_2 + \lambda_2k_1)\} + 2(k_1^2\lambda_2 + k_2^2\lambda_1)]}{2(k_1^2 + \omega^2\lambda_1^2)(k_2^2 + \omega^2\lambda_2^2)}.$$

The spectral densities are derived from (8):

$$\left|\ddot{u}_{k,n}^{\tilde{L}}\right| = \frac{\left|Q^{\tilde{L}}\right|\left|R_k\right|\omega^2 z^{-n}}{(k_1^2 + \omega^2\lambda_1^2)^{1/2}\left|F\right|}, \quad (k = 1, 2), \quad \left|Q^{\tilde{L}}\right| = \frac{2Q_0\omega_*\cos(\pi\omega/2\omega_*)}{\omega_*^2 - \omega^2}, \tag{9}$$

$$\left|F\right| = [(k_2^2 + \omega^2\lambda_2^2 - 2k_2m\omega^2 + m^2\omega^4)z + (1 - 2x)(k_2^2 + \omega^2\lambda_2^2) + 2k_2mx\omega^2 + 2\lambda_2my\omega^3]^{1/2},$$

$$\left| R_1 \right| = [k_2^2 + \omega^2 \lambda_2^2 + (k_1^2 + \omega^2 \lambda_1^2) z + 2x(k_1 k_2 + \omega^2 \lambda_1 \lambda_2) + 2y\omega(k_1 \lambda_2 - k_2 \lambda_1)]^{1/2},$$

$$\left| R_2 \right| = [(-m\omega^2 + k_1 + k_2)^2 + \omega^2 (\lambda_1 + \lambda_2)^2]^{1/2},$$

$$z = \left| e^{2i\gamma} \right| = x^2 + y^2, \quad x = x_1 + 1 - A, \quad y = y_1 + B,$$

$$y_1 = (-1)^r \sqrt{\alpha/2 + \sqrt{D}}, \quad x_1 = (-1)^r \sqrt{-\alpha/2 + \sqrt{D}}\ \text{sign}[B(1-A)], \quad r = 1, 2,$$

$$\alpha = B^2 + 1 - (1-A)^2, \quad D = \sqrt{\alpha^2/4 + B^2(1-A)^2}.$$

The value of *r* is selected so that the condition that $z \geq 1$ holds true, which corresponds to solutions decreasing at the infinity.

The boundaries of the domain of applicability for the derived analytical solutions were determined from comparing them with the finite-difference solutions of the system of equations (1), (2).

Figure 6 depicts accelerations of the 20th and 80th masses in the composite assembly with the same parameters as in Fig. 3. The solid curve is calculated by the finite difference method (explicit scheme, $\tau = 0.001$ ms), dashed curve *1* shows asymptotics (7), and *2* is for asymptotics (5). It follows from the comparison that for the composite assembly the finite-difference solution and asymptotics (5) come to a concordance much far from the point of attack ($n \sim 10$) than for the homogenous assembly ($n \sim 5$). Asymptotics (7), derived from (5) with the assumption that $n \to \infty$, satisfactorily describes the finite-difference solution results starting from $n \sim 40$. Comparing (7) and the numerical calculations indicates that the higher is the viscosity parameter, the faster the both solutions come into accordance.

In Fig. 3 there are graphs of the spectral densities of accelerations in the 3rd and 13th masses, that correspond the analytical solution (9). Analysis of the theoretical graphs yields that in the system with viscosity, similarly to the experiment, the high-frequency oscillations versus the low-frequency ones decay faster as perturbations propagate over the system. With such values of viscous parameters and when $n \geq 10$, the maximal high-frequency oscillation amplitude in the range $\Omega_2 \leq \omega \leq \Omega_3$ is less than 1 % of the maximum in the range $\omega \leq \Omega_1$.

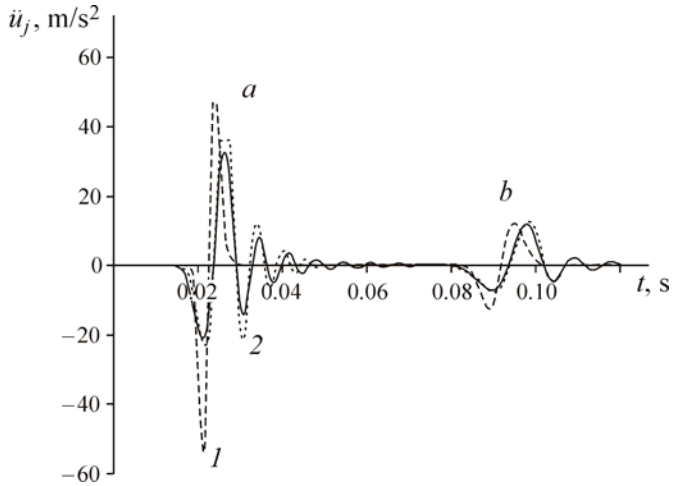

Fig. 6. Accelerations of (*a*) 20th and (*b*) 80th masses in z composite assembly with viscosity

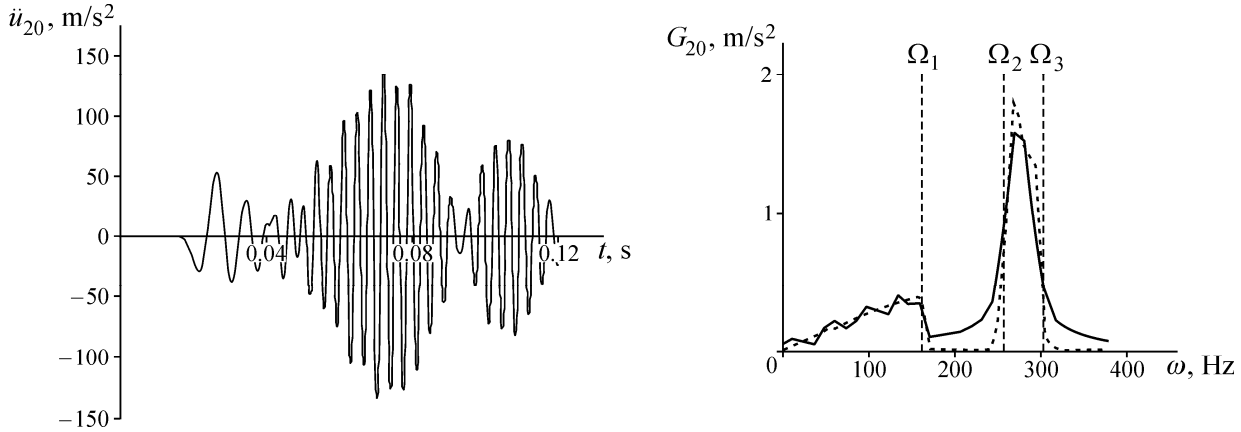

Fig. 7. Oscillogram of acceleration and the acceleration spectrum density for the 20th mass in a composite assembly, disregarding viscosity of the partings

To illustrate the effect of viscosity of partings, we performed calculations disregarding this property. Oscillograms of acceleration and the acceleration spectrum density of the 20th mass when $\lambda_1 = \lambda_2 = 0$ are presented in Fig. 7 with the other parameters as in Fig. 6. The solid curve in the graph of the acceleration spectrum densities is calculated for the finite-difference solution, the dashed curve is for analytical solution (9), and the vertical line is shows values Ω_k from (3). Comparison of the acceleration oscillograms for the 20th mass in Figs. 6 and 7 shows that viscosity causes a very strong (by orders of magnitude) decay of the high-frequency oscillations behind the quasi-front $x = c_1 t$ and a decrease of the maximal acceleration amplitude of the low-frequency pendulum wave near the quasi-front (for these parameters the reduction factor is 1.5). The same fact is confirmed by the graphs of the density spectra (Figs. 3 and 7): in the system without viscosity the high-frequency oscillations attenuate with growing n much slower than in the system with viscosity. The analytical solution presents a good qualitative and quantitative description of the spectrum densities obtained from the finite-difference solution. A slight difference in these solutions is due to the numerical dispersion.

CONCLUSION

Using an assembly of steel rods linked in turn via partings with different properties as an example, the authors have demonstrated the feasibility of modeling propagation of one-dimensional waves in block-hierarchical media based on the model of a chain of masses linked via visco-elastic springs. As a result, the authors have obtained the asymptotic regularities of a decay of the low-frequency pendulum waves excited by an impact in the second-order block-hierarchical medium with visco-elastic partings and the analytical formulas describing the spectral density of excitations in this system.

It has been determined experimentally and theoretically that when perturbations propagate over a block-hierarchical medium, both low-frequency pendulum waves and high-frequency waves arise in it. The dissipation properties of partings cause that the high-frequency waves decay quickly, the low-frequency pendulum waves attenuate faster as well. For instance, a decrease in the maximal amplitudes of velocities of masses and strains in the system with viscous partings is proportional to $t^{-1/2}$, the same decrease for the accelerations is proportional to t^{-1}; at the same time, for the system without viscosity, this proportionality is $t^{-1/3}$ and $t^{-2/3}$, respectively. It has theoretically been confirmed that given the

partings possess the viscosity, the long-wave excitations in a hierarchical medium, as in the case with ideal springs, exhibit the same asymptotical behavior as in the equivalent homogenous chain of masses with the reduced viscosity and stiffness parameters.

The study was conducted with financial support from the Russian Foundation for Basic Research, Project No. 06-05-64738, and from the Siberian Branch of the Russian Academy of Sciences, Integration Project No. 93.

REFERENCES

1. M. A. Sadovsky, "Natural lumpiness of rocks," *Dokl. AN SSSR*, **247**, No. 4 (1979).
2. M. V. Kurlenya, V. N. Oparin, and A. A. Eremenko, "Relation of linear block dimensions of rock to crack opening in the structural hierarchy of masses," *Fiz.-Tekh. Probl. Razrab. Polezn. Iskop*., No. 3 (1993).
3. M. V. Kurlenya, V. N. Oparin, and V. I. Vostrikov, "Formation of elastic wave packages in block media under impulse excitation. Pendulum-type waves V_μ," *Dokl. AN SSSR*, **333**, No. 4 (1993).
4. M. V. Kurlenya, V. N. Oparin, and V. I. Vostrikov, "Pendulum-type waves. Part I: Study of the problem and measuring instrument and computer complexes," *Fiz.-Tekh. Probl. Razrab. Polezn. Iskop*., No. 3 (1996).
5. M. V. Kurlenya, V. N. Oparin, and V. I. Vostrikov, "Pendulum-type waves. Part II: Experimental methods and main results of physical modeling, " *Fiz.-Tekh. Probl. Razrab. Polezn. Iskop*., No. 4 (1996).
6. M. V. Kurlenya, V. N. Oparin, V. I. Vostrikov, V. V. Arshavskii, and N. Mamadaliev, "Pendulu-type waves. PartIII: data of on-site observations*," Fiz.-Tekh. Probl. Razrab. Polezn. Iskop*., No. 5 (1996).
7. N. I. Aleksandrova, "Elastic wave propagation in block medium under impulse loading," *Fiz.-Tekh. Probl. Razrab. Polezn. Iskop*., No. 6 (2003).
8. N. I. Aleksandrova and E. N. Sher, "Modeling of wave propagation in block media," *Fiz.-Tekh. Probl. Razrab. Polezn. Iskop*., No. 6 (2004).
9. N. I. Aleksandrova, A. G. Chernikov, and E. N. Sher, "Experimental investigation into the one-dimensional calculated model of wave propagation in block medium," *Fiz.-Tekh. Probl. Razrab. Polezn. Iskop.*, No. 3 (2005).
10. E. N. Sher, N. I. Aleksandrova, M. V. Ayzenberg-Stepanenko, and A. G. Chernikov, "Influence of the block-hierarchical structure of rocks on the peculiarities of seismic wave propagation," *Fiz.-Tekh. Probl. Razrab. Polezn. Iskop*., No. 6 (2007).
11. L. I. Slepyan, *Non-Stationary Elastic Waves* [in Russian], Sudostroenie, Moscow (1972).
12. E. Yanke, F. Emde, and F. Lesh, *Special Functions* [in Russian], Nauka, Moscow (1968).